Scientific Research Report

Visualisation of Droplet Flow Induced by Ultrasonic Dental Cleaning

Haiyin Shu [a,1], *Xiaoyan Yu* [b,1], *Xiankun Zhu* [b], *Fan Zhang* [c], *Junjie He* [c], *Xubo Duan* [a], *Mingkun Liu* [a], *Jiachun Li* [c], *Wei Yang* [a,b,**], *Jin Zhao* [c*]

[a] *Guizhou University Medical College, Guiyang, Guizhou, China*
[b] *Guiyang Hospital of Stomatology, Guiyang, Guizhou, China*
[c] *School of Mechanical Engineering, Guizhou University, Guiyang, Guizhou, China*

ARTICLE INFO

Article history:
Received 1 November 2023
Received in revised form
10 December 2023
Accepted 22 December 2023
Available online 17 January 2024

Key words:
Respiratory infectious diseases
Droplets
Flow trajectory
Computational fluid dynamics

ABSTRACT

Introduction: During dental treatment procedures ultrasonic scalers generate droplets containing microorganisms such as bacteria and viruses. Hence, it is necessary to study the dynamic properties of generated droplets in order to investigate the risks associated with the spread of infection. The aim of this study was to visualise the flow state of droplets and to evaluate the impact of droplets generated during the use of an ultrasonic scaler during an oral surgical procedure.

Methods: We studied the spatial flow of liquid droplets through a combination of imaging and numeric simulation of a simulated dental treatment processes. First, we photographed the real time images of the ultrasonic scaler and evaluated the images using image-processing software Image J to visualise the flow of liquid droplets. Finally we simulated the flow process of liquid droplets by using the initial velocity of droplet splashing and the angle of the obtained information using computerised fluid dynamics technology.

Results: Under different working conditions, the droplet particle splashing velocity, maximum height, and spray angle varied, but the particle trajectory was generally parabolic. The maximum droplet velocity varied between 3.56 and 8.56 m/s, and the splashing height was between 40 and 110 mm.

Conclusions: During risk assessment of an ultrasonic scaler usage, difficulties arise due to the insufficient research on droplet velocity and distribution. This study aims to address this gap by visualising the flow trajectories of droplets generated by ultrasonic scalers. The obtained data will assist in developing more effective interventions based on spatial and temporal distribution of droplets. This provides a new approach for droplet particle research and offers new strategies for public health prevention and control.

Introduction

During dental diagnosis and treatment, the use of ultrasonic dental scalers as treatment instruments generates droplets of varying sizes containing organic particles (dental tissues, calculus, and dental plaque), patient blood, saliva, and other nasal and throat secretions as well as dental material fragments.[1] When patients harbour bloodborne viruses or respiratory viruses,[2] the resulting droplets can pose a significant potential risk. During diagnosis and treatment, health care workers are in close contact with patients, and when patients cough, sneeze, or undergo oral procedures involving the cutting of hard dental tissue or the use of ultrasonic instruments,

* Corresponding author. School of Mechanical Engineering, Guizhou University, Jiaxiu South Road, Huaxi District, Guiyang City, Guizhou Province, 550025, China.
** Corresponding author. Guizhou University Medical College, Xiahui Road, Huaxi District, Guiyang, Guizhou 550025, China.
E-mail addresses: vyang@gzu.edu.cn (W. Yang), zhaoj@gzu.edu.cn (J. Zhao).
Jin Zhao: http://orcid.org/0000-0002-8981-3651

[1] Haiyin Shu and Xiaoyan Yu contributed equally to this article.

https://doi.org/10.1016/j.identj.2023.12.005

their secretions, saliva, or blood may splatter onto the surrounding area.[3] Without protective measures, these droplets may directly contaminate the conjunctiva and oral and nasal mucosa of health care workers, leading to infection. In addition, aerosolised secretions, saliva, or blood can form airborne particles suspended in the air, and when patients and health care workers are exposed to an aerosolised environment for an extended period, cross-infection is likely to occur.

The concurrent utilisation of dental equipment engenders a vast spectrum of droplets characterised by a varied size distribution, with average diameters spanning from 0 to 180 um.[4,5] Concealed within these droplets lie infectious material, their presence posing threats to the well-being of health care providers and patients alike.[6,7] Due to the action of gravity, large droplets quickly fall to the ground and surface of objects.[8] Conversely, smaller droplets, endowed with a greater capacity for prolonged aerial suspension, present a consequential conduit for heightened transmission risks.[9–11] In addition, splashes and particles that fall on the surface are susceptible to further evaporation and ultimately carry the virus into the air.[12] In order to understand the spread of viruses, it is important to understand the dynamics of the droplet splashes so as to find ways to mitigate or minimise the spread of viruses by reducing their transmission pathways. Therefore, visualisation studies of droplet flow are important for assessing the risk of such infection in dentistry.

The study of aerosolised droplets generated during dental surgeries has primarily centred around investigating the microbial viability carried within these minuscule particles,[13–15] as well as assessing the size distribution of particles collected during diagnostic and therapeutic procedures.[16] Additionally, research endeavours have shed light on the spatial dispersion of droplets during such procedures and the associated exposure risks faced by health care providers.[17,18] Moreover, in order to unravel the fluid dynamics exhibited by the trajectory of these droplets as they become aerosolised, the utilisation of particle image velocimetry (PIV) systems in conjunction with computer vision techniques has emerged as a valuable tool for tracing their trajectories.[19]

In this study, during a simulated oral surgical process, the ultrasonic dental cleaning treatment images were taken, and Image J, an image-processing software, was used to process the pictures to visualise the droplet flow and to obtain data on the initial velocity of droplet particles and splash height and angle; finally, computational fluid dynamics (CFD) simulation was performed to simulate the spray process of droplet particles. The simulation results were consistent with the visualisation data in the experiment. This study not only contributes to our understanding of how droplets are spread in dental clinics, health centres, and hospitals but also provides high-quality data for visualisation of droplets in dental clinics.

Methods

To study the visualisation of droplet flow, we first photographed the droplet flow during diagnosis and treatment and processed the droplet particle flow data with Image J software. Finally, we used CFD simulation software to visualise the droplet spray process by the maximum velocity, spray angle, and other data obtained.

Experimental setup

The ultrasonic dental cleaning process was photographed in the periodontal clinic of Guanshanhu Hospital, Guiyang Stomatological Hospital, Guizhou, China, and information on the initial velocity of droplet particles, spray height, trajectory, and spray angle were obtained. The principle of ultrasonic scaler is that the high-vibration energy from the tip of the scaler atomises the mixture of coolant and saliva, and a large number of small droplets and aerosols are ejected from the oral cavity during the work, which is widely used to remove tartar deposits on teeth. In this study, the teeth in the mouth were divided into 4 zones, each including the buccal and palatal sides, for a total of 8 working conditions. There are 4 zones according to upper, lower, left, and right, which are divided into 4 zones: upper left, upper right, lower left, and lower right, bounded by the median suture of the incisors. The designations are as follows: Case 1 pertains to the buccal surface of the right maxillary, case 2 to the lingual surface of the right maxillary, case 3 to the buccal surface of the left maxillary, case 4 to the lingual surface of the left maxillary, case 5 to the buccal surface of the left mandibular, case 6 to the lingual surface of the left mandibular, case 7 to the buccal surface of the right mandibular, and case 8 to the lingual surface of the right mandibular.

During filming, the patient was placed supine on a comprehensive dental treatment table (model: 8000 Performer Operating, mode: intermittent mode, power supply: 220V −240 V, 50−60 Hz, 10 A) in the conventional position, and the filming device (Nubia Z40spro aperture: 0.35 mm focal length: F/1.65 ISO: 200 frame rate: 480 Hz) was placed on the side and directly in front of the patient for filming (Figure 1A). The temperature fluctuation interval in the room was 25 °C to 27 °C, and the relative humidity inside and outside the room was 40% to 60%. The size of the consultation room was 4.2 × 3.4 × 2.7 (L × W × H) m. The water flow rate of the ultrasonic scaler (model: PIEZON 150, power supply: 100−240 V, 50−60 Hz, 1.5 A) was approximately 40 mL/min.

Image processing

To visualise the trajectory of droplet flow, we utilised the manual tracking module of the Image J image processing software. Initially, we calibrated the starting position of the droplets, which corresponds to their initial location after being expelled from the oral cavity. Subsequently, we systematically captured the positions of these droplets in sequential frames of the image. By analysing the coordinate values of the droplet particles at each moment and calculating the time difference between adjacent frames, we approximated the maximum initial velocity of the droplets under each working condition.

By synthesising the position of the same droplet particle in different images, we constructed the flow trajectories of the droplet particles generated by the ultrasonic scaler during the treatment of different regions in the oral cavity. Figure 1B

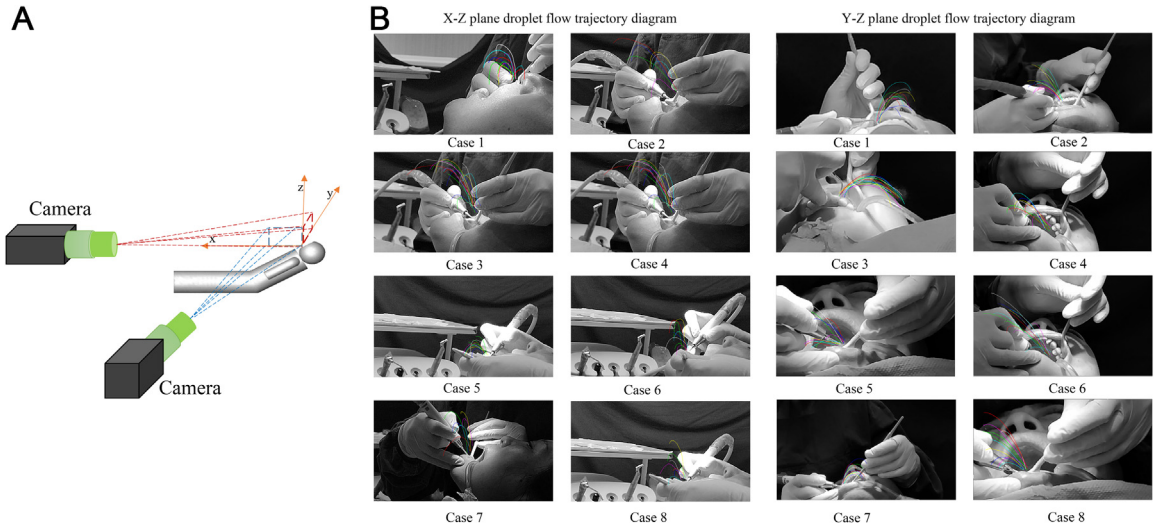

Fig. 1 – A procedure for visualising droplet aerosols generated by an ultrasonic scaler. A, Experimental setup: 2 cameras were positioned at the front and side of the chair to record the droplets produced by the ultrasonic scaler. B, Spray trajectory of droplets generated by an ultrasonic scaler, visualised through image processing with Image J software.

shows the flow trajectories obtained after processing the images using Image J software. These trajectories correspond to droplets emanating from 8 different regions of the tooth.

Computational fluid dynamics simulation

After obtaining the aforementioned data, including the initial velocity and spray angles of the droplet particles, we proceeded to employ numeric simulation techniques to investigate droplet spray phenomena. In particular, CFD was used as a preferred method to study aerodynamic problems, providing improved predictions into the indoor gas flow and particle dynamic characteristics. Using CFD, we were able to simulate and analyse the intricate dynamics associated with droplet splashing processes.

This study is a simulation of the spraying process during a dental treatment procedure, so the main study area is the area near the patient, and the geometric dimensions of the study area are 2 × 1.5 × 1.5 m. In this area, a supine patient model is set up, and the mouth part of the patient model is the source of spraying droplets. The geometric model of the human body is shown in Fig. 2A, the total length of the human model is 170 cm, the total area is 1.49 m^2, and the area of the mouth of the model is 11.46 cm^2. All velocity inlets and outlets (eg, air

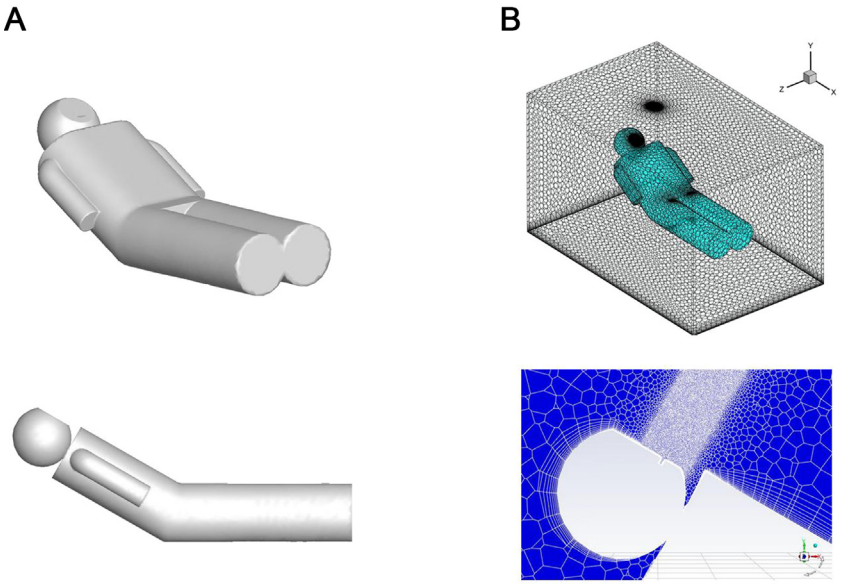

Fig. 2 – Computational fluid dynamics simulation numerical model. A, Human body geometric model. B, Model grid partitioning and local refinement.

Table – Boundary settings for different operating conditions.

Working condition	Initial velocity (m/s)	Angle between velocity direction and X-Y plane (rad)	Angle between velocity direction and X-Z plane (rad)	Jet angle (rad)
Case 1	3.56	53	−43	52
Case 2	4.48	51	49	35
Case 3	8.56	59	−43	31
Case 4	7.92	68	38	34
Case 5	4.27	43	47	52
Case 6	5.53	74	44	45
Case 7	3.64	78	−51	25
Case 8	5.36	48	50	57

The X-Y and Y-Z planes refer to the coordinate system represented in Figure 1A.
The spray was set as a cone shape. To facilitate the simulation, we used the average of the spray angles obtained in the X-Y plane and Y-Z plane from the experimental shooting as the initial parameter for the spray angle in the simulation.

inlet, air outlet, and the mouth of the human body) in the study were set as escape boundaries, and all wall surfaces (eg, the skin surface of the human body) were set as capture boundaries. Droplet particles were analysed using spheres with diameters ranging from 100 μm to 200 μm and densities of $1.2{\cdot}10^3$kg/m^3 to approximate the splash particles in the clinic.

The particle velocity obtained in the shooting experiment is utilised as airflow boundary conditions. Due to variations in the initial velocity of particle sputtering observed in each case, a simplified approach is employed to determine the initial velocity of particle sputtering. This involves calculating the arithmetic square root of the sum of the squares of velocities in the x, y, and z directions for all particles in each case. The calculation method is presented in Equation 1. Following iterative calculations using Fluent software, the resulting data were exported from the case and processed using Tecplot software, enabling visualisation of the calculated data. Additional parameters include a temperature set at 27 °C and the outlet pressure maintained at standard atmospheric levels. The average skin temperature of 34 °C is considered as the human body surface temperature. All other wall surfaces are assumed to be static, nonsliding, and adiabatic. The boundary settings under different working conditions are shown in the Table.

$$v = \sqrt{\left(\sum v_x\right)^2 + \left(\sum v_y\right)^2 + \left(\sum v_z\right)^2} \tag{1}$$

The Meshing module in Fluent was used to mesh the model, taking into account its intricate geometry. As a result, all meshes used were non-structural. To accommodate the high-speed ejection of droplet particles from the model's mouth, grid refinement was applied to the mouth and the junction between the mannequin and the flow field. Meanwhile, a coarser grid was used in other areas to control the number of grids. As a result, the simulation utilised a total of 120,000 meshes, as depicted in Figure 2B. It is worth noting that all meshes utilised in this study were nonstructural, as indicated by previous research.[20]

Turbulence is a ubiquitous natural phenomenon and an irregular fluid movement. There are various eddies of different sizes in turbulence, and the interaction between these eddies makes the analysis of turbulence difficult. The core issue of CFD prediction is how to select a suitable turbulence model to describe the physical properties of the fluid. The k-epsilon turbulence model was used for simulation in this study. This model assumes that the flow is turbulent and ignores molecular viscosity. It has good numerical stability, wide application range, low computational resource usage, and high application range accuracy. The control equation of the standard k-epsilon model is as follows.

$$\rho\frac{\partial k}{\partial t} + \rho\frac{\partial (k u_i)}{\partial x_i} = \frac{\partial}{\partial x_i}\left[\left(\mu + \frac{\mu_t}{\sigma_t}\right)\frac{\partial k}{\partial x_i}\right] + G_k - \rho\varepsilon \tag{2}$$

$$\rho\frac{\partial \varepsilon}{\partial t} + \rho\frac{\partial (\varepsilon u_i)}{\partial x_i} = \frac{\partial}{\partial x_i}\left[\left(\mu + \frac{\mu_t}{\sigma_k}\right)\frac{\partial \varepsilon}{\partial x_i}\right] + C_{1\varepsilon}\frac{\varepsilon}{k}G_k - C_{2\varepsilon}\rho\frac{\varepsilon^2}{k} \tag{3}$$

Results

Photographing the maximum velocity, maximum height, and angle of a droplet in the experiment

Figure 3A presents the maximum velocities of droplet particles under various working conditions during the oral diagnosis and treatment process. Series 1 and 2 represent velocities in the X-Z and Y-Z planes, respectively. Analysis of the data reveals that the maximum velocity in the X-Z plane is significantly higher than that in the Y-Z plane. This observation can be attributed to the predominant forward spraying of droplets during the diagnosis and treatment process. Additionally, in the Y-Z plane, the velocity distribution of droplet aerosol spraying is more concentrated, with the maximum velocity primarily falling within the range of 2 to 3 m/s, accounting for 87.5% of the total distribution.

Figure 3B displays the maximum splash heights of droplets generated by the ultrasonic scaler in different regions of the teeth, with the upper lip serving as the reference point and the highest point of the flow trajectory as the endpoint. The findings reveal that during ultrasonic scaler treatment, the droplets generated in 8 teeth regions exhibited a maximum displacement in the Z direction from the upper lip of the oral cavity, ranging from 40 to 110 mm.

Notably, in 63% of the regions, the generated droplets reached a maximum displacement in the Z direction from the upper lip within the range of 40 to 80 mm. Moreover, in zones 1, 3, and 4, the droplets generated on the palatal side of the teeth exhibited greater heights compared with those on the buccal side. The maximum horizontal displacement from the upper lip to the highest point of the droplet trajectory did not exceed

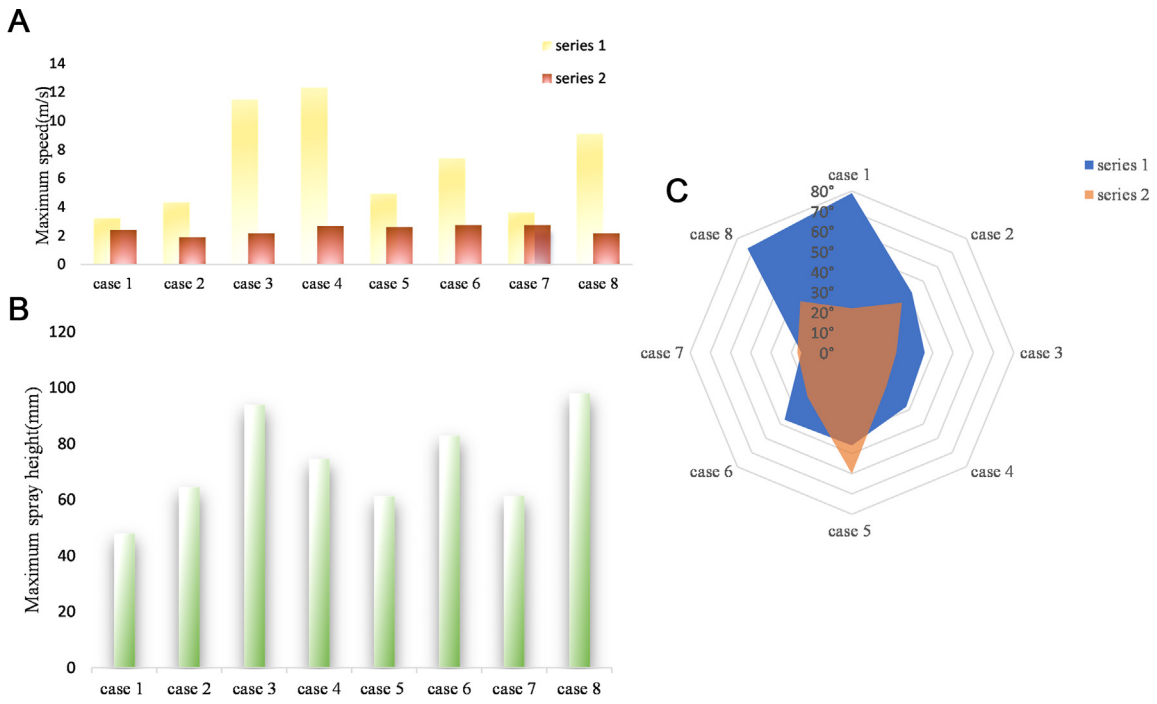

Fig. 3 – Maximum velocity, height, and ejection angle of droplets under 8 different cases and in the X-Z and Y-Z planes, as determined by data analysis. A, Quantification of maximum droplet velocity generated by ultrasonic dental cleaning machines in various regions of the teeth. B, Maximum height reached by droplets in the Z-direction at their highest point of splash. C, Initial diffusion angle of droplets: the difference between the maximum and minimum angles formed by the initial velocities of the droplets and the coordinate axis.

140 mm. specifically, in 63% of the zones, the droplets reached a maximum horizontal displacement in the X direction ranging from 40 mm to 140 mm at the highest point of their trajectory.

After undergoing image processing, the droplet flow in each region can be visually observed. Furthermore, the initial spreading angles of the droplets can be measured using the Angle tool function in Image J software. The measured values are presented in Figure 3C, where series 1 represents the spray angle in the X-Z plane and series 2 represents the spray angle in the Y-Z plane.

In the X-Z plane, the analysis reveals the following: (1) The droplets generated by the ultrasonic scaler in 8 tooth regions exhibit an initial maximum diffusion angle not exceeding 90°. (2) In 75% of the regions, the droplets have an initial maximum diffusion angle of no more than 50°, whilst in 62.5% of the regions, the initial maximum diffusion angle falls within the range of 30° to 50°. The initial diffusion angle of the droplets produced by the ultrasonic scaler is mainly distributed in this range.

Meanwhile, in the Y-Z plane, the spray angle distribution is more concentrated, ranging from 25° to 60°. Remarkably, 75% of the generated droplets have a spray angle less than 40° in this plane.

CFD simulation

CFD simulations were conducted to investigate the ambient flow field and distribution of droplet particles under various working conditions during the operation of the ultrasonic scaler. The results are presented in Figure 4, which provides a planar sectional view of the 3-dimensional field. The velocity vectors in the figure represent the magnitude of the velocity, with larger vectors indicating faster fluid flow.

From the figure, it is evident that the operation of the ultrasonic scaler generates an upward airflow, which carries the droplet particles upwards, resulting in an oblique upward direction of the airflow within the oral cavity. The airflow exhibits a clockwise or counterclockwise direction, and the droplets above the patient's face and head tend to accumulate. Therefore, additional attention should be given to implementing preventive measures in these areas. In most working conditions with high initial velocities, the spray distance of the droplets is greater.

In the X-Y plane, droplet particles with high initial velocities and large angles relative to the X-axis have a wider range of dispersion in the air. For example, conditions 4, 6, and 7 exhibit significantly larger droplet splash ranges compared with other conditions. During the initial stage of droplet splashing, the particle clusters are densely distributed, mainly concentrated above the model's head. This suggests that a majority of the droplets generated during diagnosis and treatment tend to concentrate on the patient's head. Over time, the droplets gradually disperse in all directions, and when they reach their maximum height, they begin to fall due to gravity.

And, the maximum particle velocity is located at the mouth of the model and the particles splash along the parabola to the front of the model. Meanwhile, the particle velocity decreases and then increases with the distance from the droplet entrance.

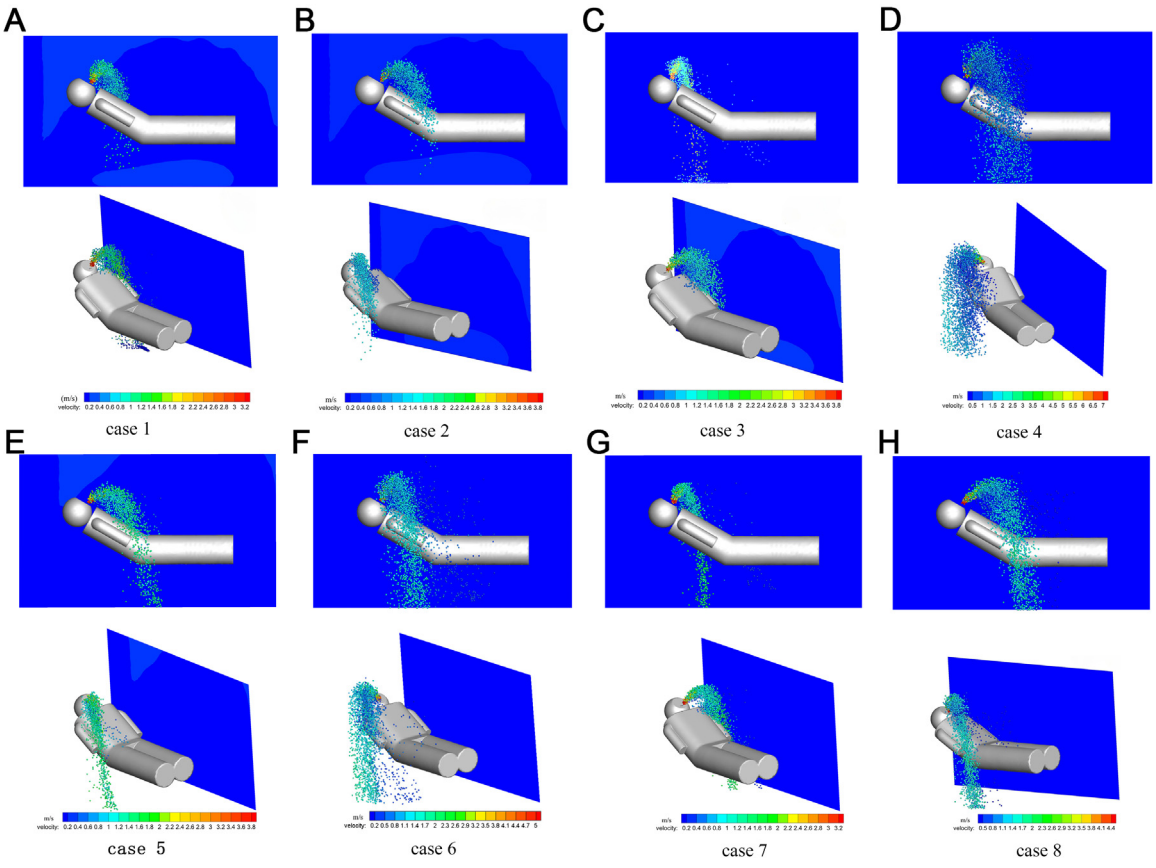

Fig. 4 – Computational fluid dynamics simulation of droplet spray trajectories and velocities generated by ultrasonic dental scaler under different working conditions.

Discussion

Ultrasonic therapy is now a routine operation in dental treatment; it has been found that the use of such equipment during treatment increases the aerosols in the office environment, .[21] Aerosols and droplets may stem from sources such as coolant water or from the patient's saliva, blood, or respiratory secretions. They act as possible agents to carry an assortment of microorganisms and bacteria.[12,22] However, previous studies have predominantly concentrated on the sedimentation characteristics of particles,[23] with little emphasis given to the examination of suspended droplets and flow fields. Moreover, the limited availability of data to precisely determine the flow velocity and droplet trajectories significantly challenges the comprehension of droplet splashing phenomena. Therefore, our research concentrated on the visualisation of splashing droplets, primarily investigating aspects such as the initial velocity of splashing particles, ejection angle, splashing height, and spatial distribution.

Our study presents a new method for exploring the spread of aerosol particles produced by ultrasonic dental scalers during dental treatment, both in vitro and in clinical environments. This approach, which is more reliable and intuitive compared to the conventional employment of microbes or tracers for analysing aerosol distribution,[13,24–26] also enables future dental aerosol research.

Research suggests that the droplets produced by ultrasonic dental cleaners can spread up to 1.2 m from the oral cavity. This finding is also corroborated by the work of Puljich et al.[27] Similarly, a study by Kaufmann et al[28] also found that these particles could still be detected at a distance of 1.1 m when using an ultrasonic dental cleaner. Additionally, research by Bentley et al[29] confirmed that aerosol splashes produced by ultrasonic cleaners can reach the patient's chest and the operator's face, which aligns with our simulation results. However, according to research conducted by Chuang et al,[30] droplets are capable of contaminating areas within a 50-cm vertical distance from the patient's mouth. This finding contradicts our own research results. The disparity could be attributed to the employment of image serialisation techniques to visualise droplet splash trajectories in our study. We specifically excluded minor droplets and prioritised larger droplets. These larger droplets exhibit more air resistance, causing them to splash a shorter distance in the vertical direction. Our results show that the trajectories of droplet splashes are parabolic, with a large number of droplet particles accumulating above the head, eventually settling and contaminating the patient's chest and oral exit area. These droplets may carry various bacteria and microorganisms.[22,31] It has been demonstrated that droplets with a larger diameter settle to the ground quicker, whereas droplets with a smaller diameter transform into "droplet nuclei" that linger in the atmosphere for a longer duration after water evaporation.[32] These droplet nuclei

can be inhaled by others, increasing the likelihood of airborne transmission of assorted infectious diseases during dental procedures. Thus, we recommend that health care providers wear masks during surgery to prevent droplet splashes and use KN95/N95 masks instead of regular surgical masks to provide a higher level of protection.

In this research, we measured the top speed of droplet particles produced during dental procedures as they exited the mouth, with rates varying from 2 to 13 m/s, aligning with earlier studies.[33] Our observations revealed that droplet splash velocity was faster in the upper left area of the mouth, plausibly attributable to right-handedness of the dentists operating the ultrasonic devices. The study of droplet velocity serves as a foundation for further analysis of droplet flow. For instance, we will utilise the particle splash velocity acquired from filming as the initial state in CFD simulations. These simulations will enable us to gain a better understanding of the droplet splash mechanism, which in turn will help us develop more effective safety measures that can reduce the spread of droplets within dental offices and mitigate the risk of infection. Additionally, the study uncovers noteworthy differences in droplet trajectory, spray angle, and exit velocity as an ultrasonic scaler functions in different sections of the mouth. These observations suggest that the droplet distribution during treatment could be linked to the instrument's working area within the oral cavity and the contact angle with teeth. Furthermore, it has been observed that droplet splatter travels not only towards the patient's front but also towards the sides. This puts dental assistants, who usually stand at the side of the patient to aid the dentist during treatment, at risk of infection.

Although the study has yielded some important results, there are still some limitations. First, in the process of visualising the droplet distribution through image serialisation techniques, we excluded some less obvious droplets, whilst some droplets of droplets that are beyond the image boundary of the droplets were not included in the study. Second, our simulation process utilised a simplified model of the human body rather than a realistic one. Whilst Nielsen's[34] study indicated that body shape had only a minor effect on indoor airflow, it remains possible that body shape could impact droplet dispersion in the vicinity of the body, necessitating further research. Furthermore, in addition to the droplets generated by ultrasonic scalers, other high-speed equipment used during dental procedures also produce a significant number of droplets. Consequently, we intend to conduct further investigations into the production of droplets resulting from the use of other high-speed dental equipment.

During the assessment of risks of using ultrasonic scalers, the process has encountered difficulties due to the lack of fundamental research on droplet velocity and distribution. Through filming and simulation, this study has achieved the visualisation of the droplet flow trajectory induced by an ultrasonic scaler. Our findings should help in the creation of more efficient protocols for managing the dental care environment, as it is based on the spatiotemporal distribution and dynamic mechanisms of droplets. This approach presents a novel means for investigating droplet particles and offers innovative strategies for public health prevention and control. This will enable us to effectively mitigate droplet transmission and safeguard the health of dental personnel and patients.

Author contributions

Haiyin Shu: conceptualisation, formal analysis, investigation, data curation, writing–original draft, writing–review and editing, visualisation, funding acquisition. Xiaoyan Yu: investigation, funding acquisition. Xiankun Zhu: investigation. Fan Zhang: methodology. Junjie He: methodology. Xubo Duan: supervision. Mingkun Liu: writing–review and editing. Jiachun Li: funding acquisition. Wei Yang: conceptualisation, methodology, formal analysis, investigation, data curation, writing–review and editing, visualisation, supervision, project administration, funding acquisition. Jin Zhao: conceptualisation, project administration. Haiyin Shu and Xiaoyan Yu contributed equally and share first authorship.

Funding

This work was supported by Guizhou Provincial Department of Science and Technology (Qiankehe support normal [2022] No. 196) and Guiyang Science and Technology Bureau (Guizhu contract [2020]-16-1).

Conflict of interest

None disclosed.

CRediT authorship contribution statement

Haiyin Shu: Conceptualization, Formal analysis, Investigation, Data curation, Writing – original draft, Writing – review & editing, Visualization, Funding acquisition. **Xiaoyan Yu:** Investigation, Funding acquisition. **Xiankun Zhu:** Investigation. **Fan Zhang:** Methodology. **Junjie He:** Methodology. **Xubo Duan:** Supervision. **Mingkun Liu:** Writing – review & editing. **Jiachun Li:** Funding acquisition. **Wei Yang:** Conceptualization, Methodology, Formal analysis, Investigation, Data curation, Writing – review & editing, Visualization, Supervision, Project administration, Funding acquisition. **Jin Zhao:** Conceptualization, Project administration.

REFERENCES

1. King TB, Muzzin KB, Berry CW, Anders LM. The effectiveness of an aerosol reduction device for ultrasonic scalers. J Periodontol 1997;68(1):45–9. doi: 10.1902/jop.1997.68.1.45.
2. Zhu S, Kato S, Yang J-H. Study on transport characteristics of saliva droplets produced by coughing in a calm indoor environment. Build Environ 2006;41(12):1691–702. doi: 10.1016/j.buildenv.2005.06.024.
3. Kohn WG, Collins AS, Cleveland JL, Harte JA, Eklund KJ, Malvitz DM. Guidelines for infection control in dental health-care settings–2003. MMWR Recomm Rep 2003;52(Rr-17):1–61. Available from: https://www.cdc.gov/mmwr/preview/mmwrhtml/rr5217a1.htm. Accessed August 25, 2023.

4. Nikitin N, Petrova E, Trifonova E, Karpova O. Influenza virus aerosols in the air and their infectiousness. Adv Virol 2014;859090:1–7. doi: 10.1155/2014/859090.
5. Mirbod P, Haffner EA, Bagheri M, Higham JE. Aerosol formation due to a dental procedure: insights leading to the transmission of diseases to the environment. J R Soc Interface 2021;18(176). doi: 10.1098/rsif.2020.0967.
6. Ge ZY, Yang LM, Xia JJ, et al. Possible aerosol transmission of COVID-19 and special precautions in dentistry. J ZhejiangUniv Sci B 2020;21(5):361–8. doi: 10.1631/jzus.b2010010.
7. Zou L, Ruan F, Huang M, et al. SARS-CoV-2 viral load in upper respiratory specimens of infected patients. New England J Med 2020;382(12):1177–9. doi: 10.1056/NEJMc2001737.
8. Cole EC, Cook CE. Characterization of infectious aerosols in health care facilities: an aid to effective engineering controls and preventive strategies. Am J Infect Control 1998;26(4):453–64. doi: 10.1016/S0196-6553(98)70046-X.
9. Hinds WC. Aerosol technology: properties, behavior, and measurement of airborne particles. New York, NY: John Wiley & Sons; 1999.
10. Cottone JA, Terezhalmy GT, Molinari JA. Practical Infection Control in Dentistry. 2nd ed. Baltimore, MD: Williams & Wilkins; 1996. p. 149–60.
11. Monaghan NP. Emerging infections implications for dental care. Br Dent J 2016;221(1):13–5. doi: 10.1038/sj.bdj.2016.486.
12. Harrel SK, Molinari J. Aerosols and splatter in dentistry: a brief review of the literature and infection control implications. J Am Dent Assoc 2004;135(4):429–37. doi: 10.14219/jada.archive.2004.0207.
13. Holloman JL, Mauriello SM, Pimenta L, et al. Comparison of suction device with saliva ejector for aerosol and spatter reduction during ultrasonic scaling. J Am Dent Assoc 2015;146(1):27–33. doi: 10.1016/j.adaj.2014.10.001.
14. Rautemaa R, Nordberg A, Wuolijoki-Saaristo K, et al. Bacterial aerosols in dental practice - a potential hospital infection problem? J Hosp Infect 2006;64(1):76–81. doi: 10.1016/j.jhin.2006.04.011.
15. Micik RE, Miller RL, Mazzarella MA, et al. Studies on dental aerobiology. I. Bacterial aerosols generated during dental procedures. J Dent Res 1969;48(1):49–56. doi: 10.1177/00220345690480012401.
16. Din AR, Hindocha A, Patel T, et al. Quantitative analysis of particulate matter release during orthodontic procedures: a pilot study. Br Dent J 2020:1–7. doi: 10.1038/s41415-020-2280-5.
17. Zemouri C, Volgenant CMC, Buijs MJ, et al. Dental aerosols: microbial composition and spatial distribution. J Oral Microbiol 2020;12(1):1762040. doi: 10.1080/20002297.2020.1762040.
18. Chanpong B, Tang M, Rosenczweig A, et al. Aerosol-generating procedures and simulated cough in dental anesthesia. Anesth Prog 2020;67(3):127–34. doi: 10.2344/anpr-67-03-04.
19. Li X, Mak CM, Ma KW, et al. Evaluating flow-field and expelled droplets in the mockup dental clinic during the COVID-19 pandemic. Phys Fluids 2021;33(4):047111. doi: 10.1063/5.0048848.
20. Corrigan A, Camelli FF, Löhner R, et al. Running unstructured grid-based CFD solvers on modern graphics hardware. Int J Numer Methods Fluids 2011;66(2):221–9. doi: 10.1002/fld.2254.
21. Leggat PA, Kedjarune U. Bacterial aerosols in the dental clinic: a review. Int Dent J 2001;51(1):39–44. doi: 10.1002/j.1875-595X.2001.tb00816.x.
22. Cristina ML, Spagnolo AM, Sartini M, et al. Evaluation of the risk of infection through exposure to aerosols and spatters in dentistry. Am J Infect Control 2008;36(4):304–7. doi: 10.1016/j.ajic.2007.07.019.
23. Timmerman MF, Menso L, Steinfort J. Atmospheric contamination during ultrasonic scaling. J Clin Periodontol 2004;31(6):458–62. doi: 10.1111/j.1600-051X.2004.00511.x.
24. Rautemaa R, Nordberg A, Wuolijoki-Saaristo K, Meurman JH. Bacterial aerosols in dental practice - a potential hospital infection problem? J Hosp Infect 2006;64(1):76–81. doi: 10.1016/j.jhin.2006.04.011.
25. Holliday R, Allison JR, Currie CC, et al. Evaluating contaminated dental aerosol and splatter in an open plan clinic environment: implications for the COVID-19 pandemic. J Dent 2021;105:103565. doi: 10.1016/j.jdent.2020.103565.
26. Yang X, Liu RL, Zhu JK, et al. Evaluating the microbial aerosol generated by dental instruments: addressing new challenges for oral healthcare in the hospital infection. BMC Oral Health 2023;23(1). doi: 10.1186/s12903-023-03109-5.
27. Puljich A, Jiao K, Lee RSB, et al. Simulated and clinical aerosol spread in common periodontal aerosol-generating procedures. Clin Oral Investig 2022;26(9):5751–62. doi: 10.1007/s00784-022-04532-8.
28. Kaufmann M, Solderer A, Gubler A, et al. Quantitative measurements of aerosols from air-polishing and ultrasonic devices: (how) can we protect ourselves? PLoS One 2020;15(12):e0244020. doi: 10.1371/journal.pone.0244020.
29. Bentley CD, Burkhart NW, Crawford JJ. Evaluating spatter and aerosol contamination during dental procedures. J Am Dent Assoc 1994;125(5):579–84. doi: 10.14219/jada.archive.1994.0093.
30. Chuang CY, Cheng HC, Yang SH, et al. Investigation of the spreading characteristics of bacterial aerosol contamination during dental scaling treatment. J Dent Sci 2014;9(3):294–6. doi: 10.1016/j.jds.2014.06.002.
31. Belting CM, Haberfelde GC, Juhl LK. Spread of organisms from dental air rotor. J Am Dent Assoc 1964;68:648–51. doi: 10.14219/jada.archive.1964.0145.
32. Kayahan E, Wu M, Van Gerven T, et al. Droplet size distribution, atomization mechanism and dynamics of dental aerosols. J Aerosol Sci 2022;166:106049. doi: 10.1016/j.jaerosci.2022.106049.
33. Sergis A, Wade WG, Gallagher JE, et al. Mechanisms of atomization from rotary dental instruments and its mitigation. J Dent Res 2021;100(3):261–7. doi: 10.1177/0022034520979644.
34. Nielsen PV. Computational fluid dynamics and room air movement. Indoor Air 2004;14(Suppl 7)):134–43. doi: 10.1111/j.1600-0668.2004.00282.x.